

Spin-phonon coupling in  $\text{ZnCr}_2\text{Se}_4$ T. Rudolf,<sup>1</sup> Ch. Kant,<sup>1</sup> F. Mayr,<sup>1</sup> J. Hemberger,<sup>1</sup> V. Tsurkan,<sup>1,2</sup> and A. Loidl<sup>1</sup><sup>1</sup>Experimental Physics V, Center for Electronic Correlations and Magnetism, University of Augsburg, D-86135 Augsburg, Germany<sup>2</sup>Institute of Applied Physics, Academy of Sciences of Moldova, MD-2028 Chişinău, Republic of Moldova

(Received 21 December 2006; published 23 February 2007)

Spin-phonon coupling and magnetodielectric effects of  $\text{ZnCr}_2\text{Se}_4$  were investigated by means of infrared (IR) spectroscopy as functions of temperature and magnetic field.  $\text{ZnCr}_2\text{Se}_4$  is dominated by ferro exchange but undergoes antiferro order at  $T_N=21$  K. In the ally ordered phase, the low-frequency IR-active phonon splits, indicating strong dynamic anisotropy via exchange interactions. Antiferromagnetic order and concomitantly the phonon splitting are wiped out by external magnetic fields. Hence,  $\text{ZnCr}_2\text{Se}_4$  is a prominent example of a spin-driven Jahn-Teller effect, which can be fully suppressed in external magnetic fields.

DOI: 10.1103/PhysRevB.75.052410

PACS number(s): 75.50.Ee, 63.20.-e, 78.30.-j

Recently, spin-phonon coupling (SPC) in materials with strong electronic correlations has gained considerable attention. The onset of low-temperature magnetic order of spins residing on a pyrochlore lattice in geometrically frustrated spinel oxides has been explained with the concept of a spin-driven Jahn-Teller effect.<sup>1,2</sup> In  $\text{ZnCr}_2\text{S}_4$  complex magnetic order results from strong bond frustration characterized by ferromagnetic (FM) and antiferromagnetic (AFM) exchange interactions of almost equal strengths.<sup>3</sup> All these compounds have in common the fact that the onset of AFM order is only accompanied by small structural distortions, hardly detectable by standard diffraction techniques, but induces a strong splitting of specific phonon modes. This phonon splitting has been experimentally verified in detail in  $\text{ZnCr}_2\text{O}_4$  (Ref. 4) and  $\text{ZnCr}_2\text{S}_4$  (Ref. 3) by optical spectroscopy. It has been explained by *ab initio* approaches, providing evidence that the dynamic anisotropy of the phonon modes is induced by the magnetic exchange alone and can be fully decoupled from lattice distortions.<sup>5,6</sup> The idea that spin-phonon interactions and the onset of magnetic order strongly influence the phonon modes had been outlined earlier by Baltensperger and Helman<sup>7</sup> and by Brüesch and D'Ambrogio.<sup>8</sup> SPC is also of prime importance in a number of multiferroic compounds and has been demonstrated for  $\text{BiFeO}_3$  (Ref. 9) and  $\text{TbMn}_2\text{O}_5$ .<sup>10</sup> In multiferroics, the strong coupling of phonons and magnons even creates an interesting class of excitations, namely, electromagnons, which are spin excitations observable by ac electric fields.<sup>11</sup>

In the normal spinel  $\text{ZnCr}_2\text{Se}_4$ ,<sup>12</sup> the Cr spins reside on the B-site pyrochlore lattice. The paramagnetic moment is close to the spin-only value of  $\text{Cr}^{3+}$ , and the susceptibility reveals a large positive Curie-Weiss (CW) temperature indicative of dominant FM exchange.<sup>13</sup> Even so,  $\text{ZnCr}_2\text{Se}_4$  reveals AFM order below 21 K. For  $T < T_N$ , the spin structure is characterized by ferromagnetic (001) planes with a turn angle of the spin direction of  $42^\circ$  between neighboring planes.<sup>14,15</sup> The magnetic moment of the  $\text{Cr}^{3+}$  ions in the spiral state is  $1.71\mu_B$ , remarkably smaller than the paramagnetic moment. This large reduction of the ordered moment has not been explained so far. The magnetic phase transition is accompanied by a small tetragonal distortion with  $c/a = 0.9992$  at 4.2 K.<sup>16</sup> The structural modulation in the vicinity of the antiferromagnetic phase transition has been investigated in detail by Hidaka *et al.*<sup>17</sup> by neutron and synchrotron

radiation, and it has been shown that magnetic and structural orders are already strongly influenced by moderate magnetic fields. It is interesting to note that magnetoelectric effects have also been reported for  $\text{ZnCr}_2\text{Se}_4$  and that the field dependence of the observed effects has been qualitatively explained by Dzyaloshinskii-Moriya type interactions.<sup>18</sup> Finally, very recently, strong spin-phonon coupling has been evidenced by the observation of a giant negative thermal expansion close to  $T_N$ , and it has been shown that antiferromagnetic order can be shifted to 0 K in external magnetic fields of 6 T.<sup>19</sup>

Here, we document SPC in  $\text{ZnCr}_2\text{Se}_4$ , which is dominated by strong FM exchange, but orders antiferromagnetically at  $T_N=21$  K.  $\text{ZnCr}_2\text{Se}_4$  belongs to a group of chromium spinels with competing FM and AFM interactions, in which the relative strength of both varies considerably with the lattice constants.<sup>20</sup> In  $\text{ZnCr}_2\text{O}_4$ , strong direct AFM exchange of Cr spins on a pyrochlore lattice determines the complex spin order at low temperatures.<sup>21</sup> In  $\text{CdCr}_2\text{S}_4$ , ferromagnetic  $90^\circ$  Cr-S-Cr exchange is responsible for a purely ferromagnetic ground state.<sup>22</sup> In  $\text{ZnCr}_2\text{S}_4$ , next-nearest-neighbor AFM exchange and  $90^\circ$  FM exchange are of equal strengths, leading to bond frustration.<sup>3</sup> In  $\text{ZnCr}_2\text{Se}_4$ , the strong FM exchange governs the ferromagnetic order within the (001) planes, but an obviously weak AFM interplane coupling is responsible for the AFM ground state and a concomitant splitting of a phonon mode, different from that observed in geometrically frustrated  $\text{ZnCr}_2\text{O}_4$ .<sup>4</sup> Because the AFM order in  $\text{ZnCr}_2\text{Se}_4$  can be shifted to  $T=0$  K in external fields of approximately 6 T,<sup>19</sup> also the mode splitting can be suppressed in external magnetic fields, resulting in spin-phonon coupling typical for ferromagnets.

Single crystalline  $\text{ZnCr}_2\text{Se}_4$  was grown by a liquid transport method from  $\text{ZnSe}$  and  $\text{CrCl}_3$  starting materials at temperatures between 900 and 950 °C. X-ray diffraction on crushed single crystals revealed a cubic single phase material with lattice constant  $a=1.0498$  nm and selenium fractional coordinate  $x=0.385$ . As shown earlier,<sup>19</sup> the magnetic susceptibility can be described by a “ferromagnetic” CW temperature of 90 K and an effective chromium moment, which is very close to the spin-only value of  $\text{Cr}^{3+}$  in an octahedral environment ( $S=3/2$ ). The reflectivity experiments were carried out in the far-infrared range using the Bruker Fourier-

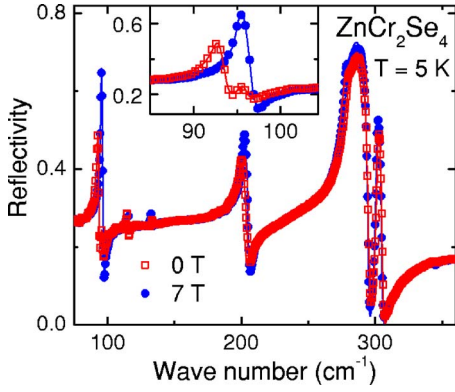


FIG. 1. (Color online) Reflectivity vs wave number of  $\text{ZnCr}_2\text{Se}_4$  at 5 K in zero magnetic field (open red squares) and in an external magnetic field of 7 T (closed blue circles). The small spikes close to 115 and 130  $\text{cm}^{-1}$  are experimental artifacts. The inset shows the wave-number regime close to phonon mode 1, which reveals a splitting in zero field. The solid lines correspond to fits as described in the text.

transform spectrometer IFS113v equipped with a He bath cryostat and a split-coil magnet for external magnetic fields of up to 7 T.

Figure 1 shows the reflectivity spectra of  $\text{ZnCr}_2\text{Se}_4$  in the range from 70 to 400  $\text{cm}^{-1}$  as measured at 5 K in external magnetic fields of 0 and 7 T. As expected from lattice symmetry, the spectrum consists of four phonon triplets of  $F_{1u}$  symmetry. The room temperature spectra agree well with those previously measured on ceramic samples.<sup>23,24</sup> The spikes between 130 and 170  $\text{cm}^{-1}$  are due to scattering processes and/or resonances in the windows of the split-coil magnet and will not be discussed further. The dielectric function  $\epsilon(\omega)$  is obtained by calculating the factorized form,

$$\epsilon(\omega) = \epsilon_\infty \prod_j \frac{\omega_{Lj}^2 - \omega^2 - i\gamma_{Lj}\omega}{\omega_{Tj}^2 - \omega^2 - i\gamma_{Tj}\omega}. \quad (1)$$

Here,  $\omega_{Lj}$ ,  $\omega_{Tj}$ ,  $\gamma_{Lj}$ , and  $\gamma_{Tj}$  correspond to longitudinal ( $L$ ) and transversal ( $T$ ) eigenfrequency ( $\omega_j$ ) and damping ( $\gamma_j$ ) of mode  $j$ , respectively. At normal incidence, the real and imaginary parts of the dielectric function,  $\epsilon'$  and  $\epsilon''$ , respectively, are related to the reflectivity via

$$R = \frac{(n-1)^2 + k^2}{(n+1)^2 + k^2}, \quad (2)$$

and the relations  $n^2 - k^2 = \epsilon'$  and  $2nk = \epsilon''$ . From the measured reflectivity, the values of  $\epsilon_\infty$ ,  $\omega_{Lj}$ ,  $\omega_{Tj}$ ,  $\gamma_{Lj}$ , and  $\gamma_{Tj}$  have been determined using a fit routine developed by Kuzmenko.<sup>25</sup> The results of these fits are shown in Fig. 1, namely, at 0 and 7 T, at a temperature of 5 K.

The temperature dependence of the eigenfrequencies of the four IR-active modes of  $\text{ZnCr}_2\text{Se}_4$  in zero external magnetic field is shown in Fig. 2 (open red squares and open red diamonds for the split modes for  $T < T_N$ ) on a semilogarithmic plot. With decreasing temperature, the phonon eigenfrequencies increase, as usually observed in anharmonic crys-

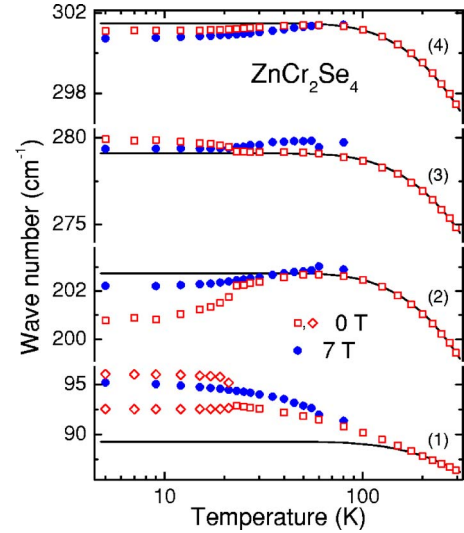


FIG. 2. (Color online) Eigenfrequencies of the phonon modes in  $\text{ZnCr}_2\text{Se}_4$  as a function of temperature. Eigenfrequencies at zero external fields (open red squares and open red diamonds) are compared to those observed at 7 T (closed blue circles). The solid lines are fits to the high-temperature results using a simple anharmonic term, Eq. (3).

tal. To get an estimate of this purely anharmonic contribution to the phonon modes, we fitted the temperature dependence assuming

$$\omega_j = \omega_{0j} \left[ 1 - \frac{c_j}{\exp(\Theta/T) - 1} \right]. \quad (3)$$

Here,  $\omega_{0j}$  indicates the eigenfrequency of mode  $j$  in the absence of spin-phonon coupling at 0 K,  $c_j$  is a mode dependent scale factor of the anharmonic contributions, and  $\Theta = 309$  K is a rough estimate of the Debye temperature, as determined from an arithmetic average of the IR-active phonon frequencies. The results of these fits to the high-temperature eigenfrequencies ( $T > 100$  K) are indicated as solid lines in Fig. 2. It is clear that all modes reveal significant deviations from this purely anharmonic behavior for  $T < 100$  K. The deviations are of the order of some percent and are positive for modes 1 and 3, but negative for modes 2 and 4. The anomalous temperature dependence smoothly evolves below 100 K, a temperature scale corresponding to the Curie-Weiss temperature  $\Theta_{\text{CW}} = 90$  K, but significantly becomes enhanced just below  $T_N$ , indicating the temperature dependence of an order parameter.

In addition to these anomalies in the temperature dependence, mode 1 reveals a clear splitting below the antiferromagnetic phase transition at  $T_N = 21$  K. This is exemplified in the inset of Fig. 1, where the results at 5 K in zero magnetic field reveal a clear two-peak structure of the reflectivity. The splitting amounts to 3.5  $\text{cm}^{-1}$  and obviously results from the breaking of cubic symmetry by the onset of the antiferromagnetic order. Already at this point, it is worth mentioning that a similar splitting of mode 2, however, has been observed in geometrically frustrated  $\text{ZnCr}_2\text{O}_4$  (Ref. 3) and a splitting of all modes has been observed in bond-frustrated

TABLE I. Eigenfrequencies  $\omega_j$  [ $\text{cm}^{-1}$ ], dielectric strength  $\Delta\epsilon_j$ , and damping  $\gamma_j$  [ $\text{cm}^{-1}$ ] for the TO phonons in  $\text{ZnCr}_2\text{Se}_4$  at 5 and 300 K in zero magnetic field.

Mode	5 K			300 K		
	$\omega_j$	$\Delta\epsilon_j$	$\gamma_j$	$\omega_j$	$\Delta\epsilon_j$	$\gamma_j$
1	92.6	0.23	1.1	86.5	0.32	3.8
	96.1	0.06	1.6			
2	200.8	0.30	5.0	199.4	0.28	6.6
3	279.9	0.94	8.0	274.9	0.93	6.8
4	301.1	0.23	2.0	297.4	0.24	3.0

$\text{ZnCr}_2\text{S}_4$ .<sup>4</sup> These observations already signal the very different spin structures that contribute to the symmetry-breaking perturbation of the dynamic properties of these spinel compounds: The oxide experiences a transition into a complex noncollinear spin structure, while the sulfide undergoes a transition into a helical spin structure like  $\text{ZnCr}_2\text{Se}_4$ , followed by a magnetic low-temperature state, where collinear and helical magnetic orders coexist.

The eigenfrequencies, dielectric strength, and damping for all IR-active TO modes are listed in Table I for 5 and 300 K. The dielectric strength has been calculated via

$$\epsilon(0) - \epsilon(\infty) = \sum_j \Delta\epsilon_j = \epsilon_\infty \left( \prod_j \frac{\omega_{Lj}^2}{\omega_{Tj}^2} - 1 \right). \quad (4)$$

In the case of nonoverlapping modes,  $\Delta\epsilon_j$  can explicitly be derived as

$$\Delta\epsilon_j = \epsilon_\infty \left( \frac{\omega_{Lj}^2 - \omega_{Tj}^2}{\omega_{Tj}^2} \right) \prod_{i=j+1}^n \frac{\omega_{Li}^2}{\omega_{Ti}^2}, \quad (5)$$

where  $n$  is the total number of IR-active phonon modes. At room temperature, the high-frequency dielectric constant has been determined to be  $\epsilon_\infty = 8.1$ , which compares reasonably with published results.<sup>23,24</sup> It is interesting to note that the dielectric strength does not strongly depend on temperature when compared to related spinel compounds and is unusually small for mode 4. The damping of modes 2 and 3 is strong even at 5 K.

The reflectivity at 5 K in an external magnetic field of 7 T is shown in Fig. 1 and is compared with the reflectivity obtained in zero external field. Only minor changes can be detected for the high-frequency modes 3 and 4, while significant shifts are obtained for phonons 1 and 2. The most spectacular observation is the splitting of mode 1, which becomes fully suppressed. This is documented in the inset of Fig. 1. We also followed the isothermal magnetic-field dependence of all modes. As an example, Fig. 3 shows phonon mode 1 at 5 K for three different fields of 0, 3, and 7 T. Already at 3 T, the AFM-derived splitting can hardly be observed and vanishes completely for 7 T. The dielectric function has been fitted for all external fields and the calculated shift of the eigenfrequencies as a function of magnetic field is shown in Fig. 4. Figures 3 and 4 provide the experimental evidence that the split branches of phonon 1 do not merge as a func-

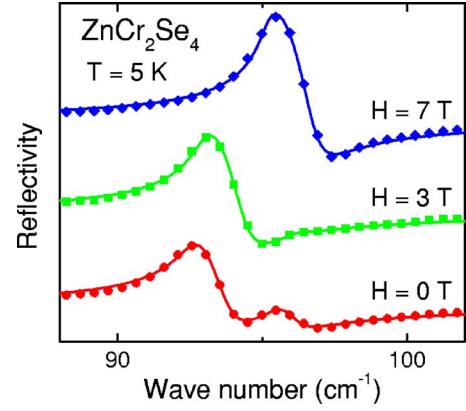


FIG. 3. (Color online) Reflectivity vs wave number for  $\text{ZnCr}_2\text{Se}_4$  around phonon mode 1 at 5 K and in magnetic fields of 0 T (red points), 3 T (green squares), and 7 T (blue diamonds). The splitting of the phonon mode becomes fully suppressed at 7 T. The lines are fits as described in the text.

tion of increasing magnetic field. The upper branch rather shows vanishing intensity for magnetic fields  $> 5$  T. Modes 1 and 2 reveal an increase, and modes 3 and 4 a decrease of the eigenfrequencies on increasing magnetic fields. This demonstrates that FM spin alignment strengthens (weakens) the force constants responsible for the phonon frequencies of the modes 1 and 2 (3 and 4). The size of the overall effect differs significantly for the different phonons and approximately amounts to 0.4, 0.3,  $-0.15$ , and  $-0.05$   $\text{cm}^{-1}/\text{T}$  for modes 1, 2, 3, and 4, respectively. Finally, in Fig. 2, we included the temperature dependence of the eigenfrequencies for all IR-active phonons as measured in external magnetic fields of 7 T. Above approximately 90 K, which corresponds to the CW temperature, magnetic-field effects are negligible. At low temperatures, the magnetic field completely suppresses the splitting of mode 1, increases the eigenfrequencies for mode 2, but decreases the frequencies for modes 3 and 4. This temperature dependence of the phonons at 7 T almost recovers the situation in ferromagnetic  $\text{CdCr}_2\text{S}_4$ .<sup>26</sup> In this compound, the frequencies of modes 1 and 2 reveal positive shifts when compared to normal anharmonic behavior, while modes 3 and 4 exhibit negative shifts. In  $\text{ZnCr}_2\text{Se}_4$  only mode 2 deviates significantly from this ferromagneticlike be-

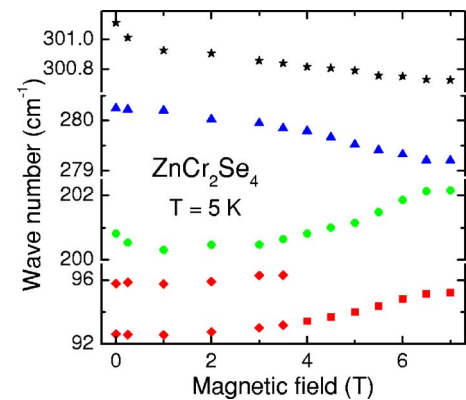


FIG. 4. (Color online) Magnetic field dependence of the phonon eigenfrequencies of  $\text{ZnCr}_2\text{Se}_4$  at 5 K.

havior. To explain the results in the ferromagnetic Cr compound, Wakamura followed the arguments of Brüesch and D'Ambrogio<sup>8</sup> and assumed that modes 1 and 2 are mainly determined by the force constants between Cr and the anions, while modes 3 and 4 are mainly governed by A-site cation-anion bonds. The former are believed to be determined by FM 90° exchange, and the latter by AFM superexchange. These arguments are compatible with our field dependent measurements. It has been pointed out by Fennie and Rabe<sup>27</sup> that the patterns of eigendisplacements may be somewhat more complex. From *ab initio* calculations, they find that in CdCr<sub>2</sub>S<sub>4</sub> for modes 1 and 2, the A-site cations move against both the B-site cations and the anions, explaining partly the low dielectric strength of these modes.

In conclusion, we have investigated the spin-phonon coupling in ZnCr<sub>2</sub>Se<sub>4</sub> by IR spectroscopy. Below  $T_N$ , we found a splitting of the lowest frequency mode, different from the findings in geometrically frustrated ZnCr<sub>2</sub>O<sub>4</sub>, where only the

second mode undergoes a splitting, and different from the observations in bond-frustrated ZnCr<sub>2</sub>S<sub>4</sub>, where all modes split. It seems evident that the Cr spinels, which have a spherical charge distribution and no spin-orbit coupling, are prone to exchange induced symmetry breaking. It is important to note that three different spinels, namely, geometrically frustrated ZnCr<sub>2</sub>O<sub>4</sub> and bond-frustrated ZnCr<sub>2</sub>S<sub>4</sub> and ZnCr<sub>2</sub>Se<sub>4</sub>, which is dominated by ferromagnetic exchange, undergo spin-driven Jahn-Teller effects with different patterns of phonon splittings. ZnCr<sub>2</sub>Se<sub>4</sub> is close to a ferromagnetic phase boundary and represents an impressive example where a spin-driven Jahn-Teller effect can be suppressed in external magnetic fields.

This work has been supported by the Deutsche Forschungsgemeinschaft (DFG) via the collaborative research center SFB 484 (Augsburg).

- 
- <sup>1</sup>Y. Yamashita and K. Ueda, Phys. Rev. Lett. **85**, 4960 (2000).  
<sup>2</sup>O. Tchernyshyov, R. Moessner, and S. L. Sondhi, Phys. Rev. Lett. **88**, 067203 (2002).  
<sup>3</sup>J. Hemberger, T. Rudolf, H.-A. Krug von Nidda, F. Mayr, A. Pimenov, V. Tsurkan, and A. Loidl, Phys. Rev. Lett. **97**, 087204 (2006).  
<sup>4</sup>A. B. Sushkov, O. Tchernyshyov, W. Ratcliff II, S. W. Cheong, and H. D. Drew, Phys. Rev. Lett. **94**, 137202 (2005).  
<sup>5</sup>S. Massidda, M. Posternak, A. Baldereschi, and R. Resta, Phys. Rev. Lett. **82**, 430 (1999).  
<sup>6</sup>C. J. Fennie and K. M. Rabe, Phys. Rev. Lett. **96**, 205505 (2006).  
<sup>7</sup>W. Baltensperger and J. S. Helman, Helv. Phys. Acta **41**, 668 (1968); W. Baltensperger, J. Appl. Phys. **41**, 1052 (1970).  
<sup>8</sup>P. Brüesch and F. D'Ambrogio, Phys. Status Solidi B **50**, 513 (1972).  
<sup>9</sup>R. Haumont, J. Kreisel, P. Bouvier, and F. Hippert, Phys. Rev. B **73**, 132101 (2006).  
<sup>10</sup>R. Valdés Aguilar, A. B. Sushkov, S. Park, S.-W. Cheong, and H. D. Drew, Phys. Rev. B **74**, 184404 (2006).  
<sup>11</sup>A. Pimenov, A. A. Mukhin, V. Yu. Ivanov, V. D. Travkin, A. M. Balbashov, and A. Loidl, Nat. Phys. **2**, 97 (2006); A. Pimenov, T. Rudolf, F. Mayr, A. Loidl, A. A. Mukhin, and A. M. Balbashov, Phys. Rev. B **74**, 100403(R) (2006).  
<sup>12</sup>H. Hahn and K.-F. Schröder, Z. Anorg. Allg. Chem. **269**, 135 (1952).  
<sup>13</sup>F. K. Lotgering, Proceedings of the International Conference on Magnetism, Nottingham, England, 1964 (The Institute of Physics and the Physical Society, University of Reading, Berkshire, England, 1965), p. 533; Solid State Commun. **3**, 347 (1965).  
<sup>14</sup>R. Plumier, C. R. Acad. Sci. URSS **260**, 3348 (1965); J. Phys. (Paris) **27**, 213 (1966).  
<sup>15</sup>J. Akimitsu, K. Siratori, G. Shirane, M. Iizumi, and T. Watanabe, J. Phys. Soc. Jpn. **44**, 172 (1978).  
<sup>16</sup>R. Kleinberger and R. de Kouchkovsky, C. R. Seances Acad. Sci., Ser. B **262**, 628 (1966).  
<sup>17</sup>M. Hidaka, N. Tokiwa, M. Fujii, S. Watanabe, and J. Akimitsu, Phys. Status Solidi B **236**, 9 (2003); M. Hidaka, M. Yoshimura, S. Takahashi, S. Watanabe, and J. Akimitsu, *ibid.* **236**, 209 (2003); M. Hidaka, M. Yoshimura, N. Tokiwa, J. Akimitsu, Yong Jun Park, Jae Hyun Park, Sung Dae Ji, and Ki Bong Lee, *ibid.* **236**, 570 (2003).  
<sup>18</sup>K. Siratori and E. Kita, J. Phys. Soc. Jpn. **48**, 1443 (1980).  
<sup>19</sup>J. Hemberger, H.-A. Krug von Nidda, V. Tsurkan, and A. Loidl, cond-mat/0607811 (unpublished).  
<sup>20</sup>P. K. Baltzer, P. J. Wojtowicz, M. Robbins, and E. Lopatin, Phys. Rev. **151**, 367 (1966).  
<sup>21</sup>S.-H. Lee, C. Broholm, W. Ratcliff, G. Gasparovic, Q. Huang, T. H. Kim, and S.-W. Cheong, Nature (London) **418**, 856 (2002).  
<sup>22</sup>J. Hemberger, P. Lunkenheimer, R. Fichtl, H.-A. Krug von Nidda, V. Tsurkan, and A. Loidl, Nature (London) **434**, 364 (2005).  
<sup>23</sup>H. D. Lutz, G. Wäschenbach, G. Kliche, and H. Haeuserler, J. Solid State Chem. **48**, 196 (1983); J. Zwinscher and H. D. Lutz, J. Solid State Chem. **118**, 43 (1995).  
<sup>24</sup>K. Wakamura, T. Arai, and K. Kudo, J. Phys. Soc. Jpn. **40**, 1118 (1976).  
<sup>25</sup>A. Kuzmenko, RefFIT, Version 1.2.44, University of Geneva, 2006, <http://optics.unige.ch/alexey/refit.html>.  
<sup>26</sup>K. Wakamura and T. Arai, J. Appl. Phys. **63**, 5824 (1988).  
<sup>27</sup>C. J. Fennie and K. M. Rabe, Phys. Rev. B **72**, 214123 (2005).